

Solid State Detection of Low Energy Ions and Electrons for Constellation Missions

S. M. Ritzau, H. O. Funsten and J. E. Borovsky

Space and Atmospheric Sciences Group, Los Alamos National Laboratory, Los Alamos, NM

Abstract. A constellation mission will seek to provide the maximum scientific return from a minimal set of simple, low mass and power instruments. We investigate the use of solid state detectors in minimum resource space plasma analyzers for low (<50keV) energy particles.

1. Introduction

Small-satellite and multiple-satellite missions are likely to be a wave of the future in magnetospheric physics. The development of plasma detectors that use a minimum of spacecraft resources is essential for the success of future multi-satellite missions such as Magnetospheric Multiscale and Magnetospheric Constellation [Burch *et al.*, 1997]. These missions will be required to measure plasma properties with high time resolution on multiple satellites to obtain the goals of mapping global plasma flows, studying turbulence in the magnetosphere, investigating the mechanisms of plasma entry into the magnetosphere, and discerning the roles that the aurora plays in the magnetosphere [e.g. Vondrak, 1998].

Traditionally, space plasma measurements have utilized three types of instruments to measure ion and electron distributions: solid state detectors (SSDs) for particle energies greater than ~100 keV [e.g. Belian *et al.* 1981], electrostatic energy analyzers for particles with energies less than ~40 keV [e.g. Young *et al.* 1998], and retarding field analyzers/Faraday cups for particles with energies less than several keV [Bridge *et al.*, 1960]. To cover a broad energy range from several eV to >100 keV, at least two instruments are required; typically, an electrostatic energy analyzer is used in addition to a SSD. However, a mission with highly constrained resources, which would be applicable to a constellation mission, requires instrumentation having a high scientific return, while utilizing an absolute minimum of spacecraft resources. A clear advance for electron and ion measurements is a single instrument that would detect and measure the energy of ions and/or electrons over a broad energy range. This study investigates the feasibility of using a single SSD to detect ions and electrons at energies less than 20 keV.

2. Particle Detection Using Solid State Detectors

Solid state detectors are simple, compact, and robust devices that measure the energy deposited by an incident ion or electron. They have been used extensively to measure particle distributions in space, for example, the CEPPAD instrument on POLAR [Blake *et al.*, 1995]. We first review the fundamental operation of SSDs and consider their detection of ions and electrons at energies <50 keV.

2.1 Introduction

Energetic ions and electrons lose energy in a solid primarily in two ways; in collisions which impart energy to the electrons of the solid (*electronic* collisions) and in interactions with the target nuclei (*nuclear* collisions.) The total energy lost to electronic collisions E_E is directed primarily into the production of electron hole (e-h) pairs - "freed" elec-

trons and the empty states they leave behind. The mean number of e-h pairs generated is $N_{eh} = E_E/e$, where e is the accepted mean pair creation energy. Once freed, the electrons will diffuse or respond to the influence of an electric field until they are collected, trapped, or annihilated by recombination with a hole.

Solid state detectors (SSDs), which are essentially reverse-biased diodes with parallel planar electrodes, have an electric field in the depletion layer that quickly separates the e-h pairs produced by ionizing radiation within this layer. This bias drastically reduces the chance for recombination and allows enough time for these charges to be collected to produce an output current (or charge pulse) with a magnitude that is proportional to E_E . Since e is small (for Si, $e \approx 3.7$ eV [Wu and Wittry, 1978, Funsten *et al.*, 1997]) a single particle at an incident energy of 1 keV can produce several hundred e-h pairs.

SSDs designed for use at higher energies ($E > 50$ keV) often have metalized contacts on their entrance surfaces to allow for an external electric field to be applied to the devices. This speeds up the separation of charge and further reduces the probability of electron recombination before collection. Furthermore, the accompanying reduction in capacitance of the detector also increases the output voltage of the detector, which will strongly affect the low-energy detection threshold when using the detector in pulse-counting mode. Typically the metalized contacts are sufficiently thick to make the particles insensitive to visible and UV light.

Many SSDs have passivation layers at their surface to render them chemically inert and to minimize leakage currents. These layers, which are usually SiO_2 or SiN_x , may be several hundred Ångströms thick and can affect the collection of electron hole pairs in two ways. First, e may be quite high in the passivation layer (e.g. ~17 eV for SiO_2 [Ausman and McLean, 1975]), which significantly reduces the number of e-h pairs created per unit energy loss of the particle in the layer. Second, a potential well near the surface can trap charges, resulting in eventual recombination [Nikzad *et al.*, 1998]. One method to reduce the impact of surface recombination is the use of a highly doped (d-doped) region at the surface to terminate surface drift fields [Nikzad *et al.*, 1998]. This allows for increased collection efficiency of the charge created near the detector surface and thus an increase in the pulse magnitude for low energy particles.

Several fundamental parameters of a SSD will govern their performance and lifetime. First, noise in the SSD can severely limit the low energy threshold for detection of ions or electrons. Sources of intrinsic SSD noise include a "dark current," which is due to thermal promotion of carriers across the depletion region, and reverse-leakage currents, which can be significant if large biases are applied to the detector.

Second, the energy resolution of a SSD is limited by the statistical variation of the total number N_{eh} of e-h pairs created. The variance in N_{eh} is given by $2.35(F/N)^{1/2}$ where F is the Fano factor. For $F = 0$ every incident particle produces the same number of e-h pairs. For $F = 1$ the interactions of the incident projectile within the solid are completely random, so the variance follows Poisson statistics. A value of $F < 1$ infers that sequential interactions of an incident ion or electron in the detector are correlated. Typical values of F for Si SSDs are ~0.1

[Zullinger et al., 1970].

Third, the detector lifetime is governed by damage induced by energetic particles. The primary damage mechanism is the production of recombination sites by nuclear collisions [Ritzau et al., 1998]. The most common type of damage produced is a *Frenkel-pair*, which is an interstitial atom and its corresponding vacancy. Detailed Monte Carlo simulations by De La Rubia [1995] show that vacancy and interstitial clustering may be the controlling factor in detector damage.

A variety of techniques can be used to make SSDs capable of imaging. These include the fabrication of strip detectors [e.g. Litke and Schwarz, 1995], the use of charge-coupled devices (CCDs), and hybrid-detectors [Fossum et al., 1998].

2.2 Solid State Detectors at Low (keV) Energies

A recent advance in SSD fabrication led to fabrication of a p-n junction silicon photodiode having virtually no recombination of radiation at the Si-SiO₂ interface [Canfield et al., 1989, Korde and Geist, 1989, Korde et al., 1993]. These diodes have a thin (60 Å) passivating oxide window that enables near-theoretical quantum efficiency measurements for EUV photons. Since the energy loss of an incident ion or electron in the window is small and the surface recombination is minimal, these diodes have also been used to study the low energy detection limits of ions and electrons incident on Si-based SSDs.

The experimental method is described in detail in Funsten et al. [1997]. A Faraday cup was used to measure an ion or electron beam with incident energy E_0 . The photodiode, which was operated without external bias, was then moved into the beam, and the photodiode current I_{PD} was measured. The beam current was then measured a second time, and the average beam current I_0 of the two measurements was obtained.

Each diode produced a “dark current” I_D due to thermal promotion of carriers across the depletion region. This current, which was subtracted from I_{PD} to determine the photodiode responsivity, was measured before and after each measurement of I_{PD} . Additionally, the dark current was measured periodically during irradiation of the photodiode since it increased with increasing ion fluence.

The photodiode responsivity R is a measure of the number of collected electron-hole pairs created in the active region of the photodiode relative to the total energy deposited by that particle in the detector. For our experiments, the measured responsivity R is defined as

$$R = \frac{I_{PD} - I_D}{E_0(I_0/e)} \quad (1)$$

which was derived using the electron charge e and the measured values I_{PD} , I_D , E_0 , and I_0 . Assuming 100% collection efficiency of electrons and holes produced in the device, which is a good approximation due to the unique photodiodes used here, R can be related to the number N_{eh} of e-h pairs created using the expression

$$N_{eh} = RE_0 \quad (2)$$

At high energies for which almost all energy is lost by the incident particle to electronic collisions in the active region of the detector, we obtain $R \gg 1/e$. Deviations in R from a value of $R = 1/e$, caused for example by energy lost to nuclear collisions, are commonly referred to as the energy defect [Steinberg et al., 1972, Finch et al., 1979].

Figure 1 shows the number of electron hole pairs created by incident electrons, H⁺, He⁺, and O⁺ as a function of incident energy. The ideal case, for which $N_{eh} = E_0/e$ is depicted as a solid line using a value for the mean electron-hole pair creation energy e of 3.7 eV for Si. Also shown in Figure 1 is a dashed horizontal line corresponding to the minimum detection threshold (500 electrons) for typical existing elec-

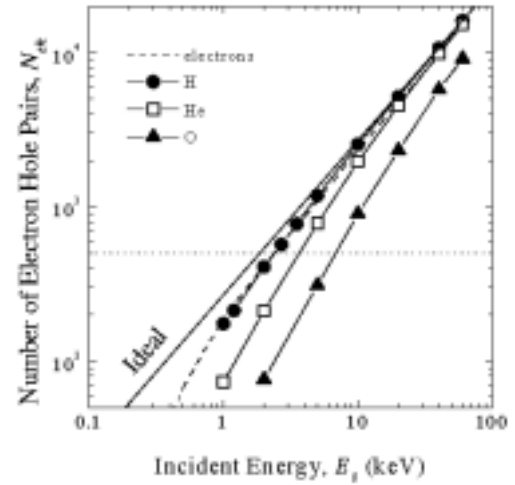


Figure 1. Measured response of SSD to incident ions and electrons indicating the mean number of e-h pairs created by a particle of a particular energy and species. The horizontal line corresponds to the detection limit (500 electrons) of typical electronics.

tronics. These measurements were made in current mode with high capacitance detectors, so that the horizontal line does not represent an achieved energy resolution. The threshold instead represents the approximate detection for a Si detector. Using 500 electrons as the minimum detectable pulse, Figure 1 infers that SSDs could be used to detect ~ 2 keV H, ~ 2 keV electrons, and ~ 7 keV O.

As mentioned previously, energy lost to nuclear processes does not contribute directly to the output signal and damages the detector, thereby degrading its performance. In these cases, the responsivity decreases in an approximately exponential fashion with increasing ion fluence due to increased damage in the photodiode. This exponential decrease was observed for all incident ion species used here, so we fit the data using

$$R_M(\Phi) = R_M(0)e^{-\Phi/\Phi_D} \quad (3)$$

where Φ is the incident ion fluence and Φ_D is a characteristic damage fluence that is dependent on the incident ion species and energy. Values of Φ_D , which are inversely proportional to the damage cross section [Ritzau et al., 1998], are shown as a function of incident energy for several ion species in Figure 2. Values of Φ_D range from $\sim 4 \times 10^{13}$ cm² for 10 keV H⁺ to $\sim 7 \times 10^{10}$ cm² for 60 keV Ar⁺. Electrons in the energy range 0.2–40 keV did not damage the SSDs at fluxes of 10^{14} e/cm² [Funsten et al., 1997]. An expected number of counts that a SSD would measure during a three year mission (assuming $\sim 10^4$ ions s⁻¹) is $\sim 10^{12}$ counts. For a 0.5cm² detector, this is considerably less than the characteristic damage fluence for H ($\sim 10^{13}$ cm²).

These damage fluences are important for photodiodes similar to those used in this study, in which one contact is located at the periphery of the device. Electrons created in the depletion region travel toward the contact through a long channel located parallel to and immediately behind the SiO₂ photodiode surface [Ritzau et al., 1998.] Therefore, electrons could travel a significant distance through damaged material, greatly enhancing their recombination probability. A photodiode with this geometry has an intrinsically high capacitance and would only be used in applications requiring current measurements.

For a SSD operated in pulse counting mode, this channel would not exist since the front of the SSD consists of a conductive contact. Electrons are immediately collected and do not traverse a channel, so the characteristic damage fluence Φ_D shown in Figure 2 is a gross overes-

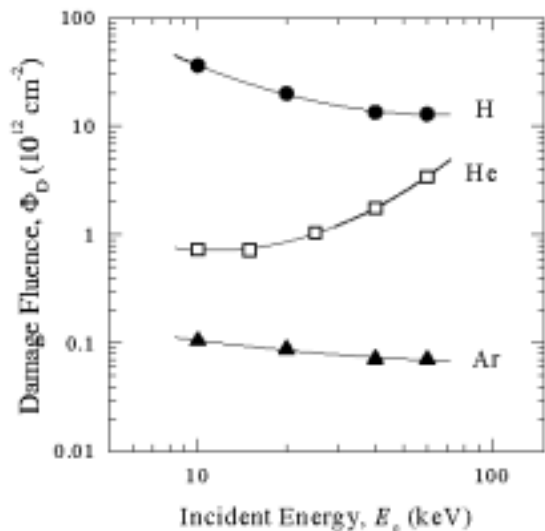


Figure 2. The damage fluence Φ_D , derived from a fit of Eq. 3 to the data is shown as a function of incident ion energy E_i . Φ_D is inversely proportional to the damage cross section s_D [Ritzau et al., 1998].

timate of the damage to these devices. For a SSD in pulse counting mode, damage resulting in decreased series resistance may be more important than recombination of electrons or holes.

2.3 Elimination of Background Light Contamination.

Solid state detectors capable of measuring particles with a few keV are also sensitive to light. Typically a SSD uses a relatively thick (e.g., 500-800 Å) window of a specific material (e.g. Al) to attenuate the light. However, this will not work for energies less than ~20 keV since the window thickness must be thicker than a typical particle range to effectively attenuate the photon signal. Similarly, foils of sufficient thickness placed in front of the detector to block the light will also stop heavy keV particles. Recently, an extensive survey of methods for blocking the UV/EUV flux was conducted [Gruntman, 1997]. We mention only a few techniques here.

If the particles are charged, electrostatic or magnetic deflection can be used to separate the incident ions and photons. For incoming neutrals, or cases where a straight-through path is required, the particles can be ionized by passage through a thin foil and then separated in the same manner as ions. This process is, however, inefficient for ions with a few keV [Funsten et al., 1993], and will cause significant angular and energy scattering of the ions.

Diffraction-based filtering offers a way of attenuating the light signal without affecting the energy or trajectory of the incoming particle. This form of filtering relies on the attenuation of the photons by features in the filter which are much smaller than the photon wavelength. These filters have been made in the form of perforated foils [Gruntman, 1997] and free-standing diffraction gratings [VanBeek, 1998]. The perforated foils are of limited use due to their low geometric transparency, but the diffraction gratings have been shown to reduce the H Ly- α (1216 Å) emission by a factor of $\sim 5 \times 10^{-6}$ while maintaining ion transmissions of $\sim 8\%$. These gratings polarize, but do not effectively attenuate, visible light so a second, larger featured grating with a perpendicular polarization axis would be needed to provide light rejection over a full range of wavelengths.

For a $\sim 100\%$ carrier collection efficiency photodiode with a transparent window, the background current signal due to light would be

$$I_b \approx \frac{Ae}{\epsilon} \int_{\epsilon}^{\infty} d\nu h\nu \phi(\nu) \quad (4)$$

where A is the detector area, $h\nu$ is the photon energy, and ϕ is the photon flux. As an example of a typical signal level, the response of a photodiode with 100% carrier collection efficiency to the photon flux from the airglow of the earth is shown in Figure 3. The incident spectrum is adjusted to nadir-viewing from 200 km at midmorning [Meier, 1991]. With the use of a single, free-standing, 0.5 μm thick gold grating with a slot width of 50 nm and a 200 nm period, the current due to photons with wavelengths $\lambda < 2000$ Å is significantly reduced. Also shown in Figure 3 are the transmitted signal through the free-standing grating previously described and through a second 1.0 μm thick gold blocking grating with 250 nm slots and a 500 nm period. The latter grating further reduces the photon flux by acting as a crossed polarizer.

3. Detector Concepts for a Minimum Resource Constellation Mission

The level of complexity of any instrument for a constellation mission is likely to be inversely related to the number of spacecraft (*i.e.* more spacecraft, fewer resources and simpler instrumentation.) As mentioned previously, SSDs can be operated in either current mode, in which the detector acts as an amplifier for input currents, or in pulse mode, in which each incident particle generates a discrete pulse having a magnitude that is dependent on the particle energy. We discuss each mode separately.

3.1 Particle Detection by Current-Mode Operation

For an application in which noise due to ambient light is small, a SSD can be used as a sensitive Faraday cup. In this configuration, the

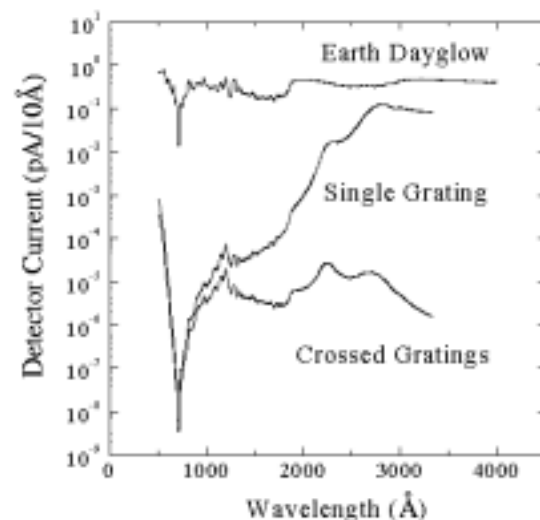


Figure 3. The spectral response from Sun and Earth's albedo using a 100% internal carrier collection efficiency photodiode for three cases; a bare photodiode (top $I_b = 1.270$ nA), a diode with a UV-blocking nano-structure grating (middle, $I_b = 150$ pA), and a diode behind a pair of crossed gratings (bottom, $I_b = 0.11$ pA). The 0.5 μm thick gold nano-structure grating has a period of 200 nm and a slot width of 50 nm. The other 1.0 μm thick gold grating has a period of 500 nm and a slot width of 250 nm. The spectral data is from Meier [1991].

current of ions or electrons at an incident energy E_0 is amplified by a factor of

$$\frac{I_{PD}}{I_0} = \frac{E_0 + qV_B}{e} R \quad (5)$$

The entire the detector could be biased to a potential V_B to accelerate the incident charged particle into the detector. This would increase the energy of the particle at the detector by qV_B , and would therefore further amplify the input current I_0 . Because of amplification, SSD-based detectors could be made considerably smaller than existing Faraday cups and still maintain the same sensitivity.

In areas where the background light intensity is strong enough to pollute the measurement, freestanding diffraction gratings could be used to suppress this background as outlined in section 2.3. A voltage applied to the UV-blocking grating would allow operation as a Faraday cup or as retarding potential analyzer.

An array of these devices could be used at the exit of a toroidal "top hat" electrostatic analyzer [Young *et al.*, 1988] to image a plasma distribution over a 2π radian field of view.

3.2 Particle Detection in pulse mode operation

The most meaningful space plasma measurements provide information about an ion's mass, energy, charge state, and incident direction. For a minimum resource or constellation mission, these measurements must be obtained under highly constrained spacecraft resources including mass, volume, and power, which likely eliminates even simple time-of-flight mass spectrometers.

SSD-based instrumentation to measure E and q utilizes an electrostatic analyzer to measure E/q and a SSD to determine E [Gloeckler, 1983]. The detector may be biased negatively to several tens of kV to enhance the detection efficiency of low energy ions. To make simultaneous energy distribution measurement of both ions and electrons, an electrostatic analyzer which uses a nested-hemisphere as outlined by Funsten and McComas [1998] could be used (See Figure 4.)

Additionally, position information could be gathered from the use of a strip detector [e.g. Litke and Schwarz, 1995] or a hybrid detector [e.g. Fossum *et al.*, 1998] at lower energies. At high enough energies, ion mass can be obtained by a detector consisting of a series of SSDs in series of layers [e.g. Wilken *et al.*, 1997]. At each layer, the energy loss of the ion is measured, and the cumulative energy loss throughout all layers is E_0 . Once E_0 is derived, the mass is obtained using the relative magnitudes of the energy lost in each layer, which is dependent on the ion mass.

4. Summary

Solid state detectors are simple, compact, robust detectors which have a long history of use in space. New detector technologies, coupled with novel instrument designs make these detectors uniquely suited to measurement of low-energy ions and electrons for constellation missions.

To further determine the viability of these detectors at low energies, we have measured the responsivity and damage characteristics of silicon-based SSDs under bombardment by 3-60 keV ions.

Because SSDs sensitive to low energy ions will also be sensitive to light, we review some light rejection techniques including the use of freestanding UV-blocking gratings. We have also presented a handful of possible applications for SSD-based instruments intended to measure space plasmas including miniaturized Faraday cups, retarding potential analyzers, E and q analyzers, and position-sensitive detectors.

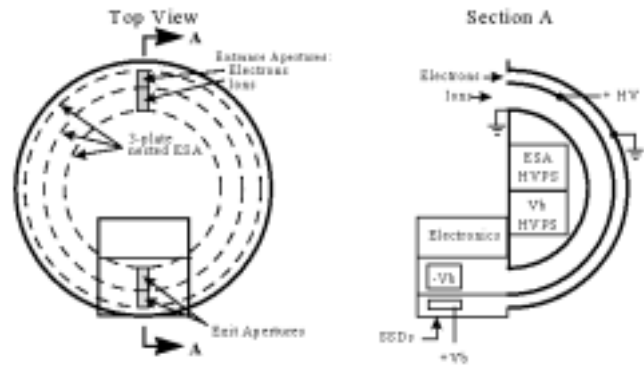


Figure 4. Schematic diagram of a space plasma instrument capable of measuring E and q for ions and electrons, consisting of an electrostatic energy analyzer and two solid state detectors (one ions and one for electrons). Particles are sorted by E/q in the electrostatic analyzer. The electrons can be measured by the SSD in current mode since their charge q is known.

Acknowledgments. This work was performed under the auspices of the United States Department of Energy. The authors gratefully acknowledge discussions with Bruce Barraclough, Dick Belian, Ron Harper, Raj Korde, Geoff Reeves, and John Steinberg.

REFERENCES

- Ausman, G.A., and F.B. McLean, Electron-Hole Pair Creation Energy in SiO_2 , *Appl. Phys. Lett.*, 26, 173-175 1975.
- Belian, R.D., *et al.*, Timing of energetic proton enhancements relative to magnetoteric substorm activity and its implication for substorm theories, *JGR*, 86, 1415, 1981.
- Blake, J.B., *et al.*, CEPPAD: Comprehensive Energetic Particle and Pitch-Angle Distribution Experiment on POLAR, *Space Sci. Rev.*, 71, 531-562, 1995.
- Bridge H.S., *et al.*, An Instrument for the Investigation of Interplanetary Plasma, *J. Geophys. Res.* 65, 3053-3055, 1960.
- Canfield, L.R., *et al.*, Stability and Quantum Efficiency Performance of Silicon Photodiode Detectors in the Far Ultra-Violet, *Appl. Opt.*, 18, 3940-3943, 1989.
- Burch, J.L., *et al.*, Sun-Earth Connection Roadmap: Strategic Planning for the Years 2000-2020, NASA Office of Space Science, Washington, D.C., 1997.
- Korde R., and J. Geist, Quantum Efficiency Stability of Silicon Photodiodes, *Appl. Opt.*, 26, 5284-5290, 1989.
- Korde R., J. Cable, and R. Canfield, 100% Internal Quantum Efficiency Silicon Photodiodes with One G-Rad Passivating Silicon Dioxide, *IEEE Trans. on Nuc. Sci.*, 40, 1655-1659, 1993.
- Diaz de la Rubia, T., and G.H. Gilmer, Structural Transformations and Defect Production in Ion-Implanted Silicon: A Molecular Dynamics Simulation Study, *Phys. Rev. Lett.*, 74, 2507-2510, 1995.
- Finch E.C., *et al.*, Plasma and Recombination Effects in the Fission Fragment Pulse Height Defect in Surface Barrier Detectors, *Nucl. Instr. Meth.*, 163, 467-477, 1979.
- Funsten, H. O., *et al.*, Shell Effects Observed in Exit Charge State Distributions of 1-30 keV Atomic Projectiles Transiting Ultra-Thin Carbon Foils, *Nuc. Instr. Meth. B*, 80/81, 49-52, 1993.
- Funsten, H. O., *et al.*, Response of 100% Internal Quantum Efficiency Silicon Photodiodes to 200 eV - 40 keV Electrons, *IEEE Trans. Nuc. Sci.*, 44, 2561-2565, 1997.
- Funsten, H.O., and D.J. McComas, Limited Resource Plasma Analyzers: Miniaturization Concepts, in *Measurement Techniques in Space Plasmas: Particles*, ed. By R.F. Plaff, J.E. Borovsky, and D.T. Young, Amer. Geophys. Union, Wash., DC, 1998.
- Gloeckler, *et al.*, The Solar Wind Ion Composition Spectrometer (SWICS), ESA SP-1050, 77-103, 1983.
- Gloeckler, *et al.*, The Solar Wind Suprathermal Ion Composition Investigation on the WIND Spacecraft, *Space Sci. Rev.*, 79-124, 1992.
- Gruntman, M., Energetic Neutral Atom Imaging of Space Plasmas, *Rev. Sci. Instr.*, 68 (10), 3617-3656, 1997.

- Litke A., and A. Schwarz, The Silicon Strip Detector, *Sci. Amer.*, 272, 76-81, 1995.
- Meier, R. R., Ultraviolet Spectroscopy and Remote Sensing of the Upper Atmosphere, *Space Science Reviews*, 58, 1-185, 1991.
- Nikzad, S., *et al.*, Delta-Doped CCDs as Low-Energy Particle Detectors, NASA Tech Briefs, NPO-20178, NPO-20153, 48-50, 1998.
- Ritzau, S. M., *et al.*, Damage Induced in 100% Carrier Collection Efficiency Silicon Photodiodes by 10-60 keV Ion Irradiation, *IEEE Trans. Nucl. Sci.*, submitted Sept. 1998.
- Steinberg, E.P., *et al.*, Pulse Height Response Characteristics for Heavy Ions in Surface Barrier Detector, *Nucl. Instr. Meth.*, 99 309-320, 1972.
- Van Beek, *et al.*, Nano-scale Freestanding Gratings for UV Blocking Filters, *J. of Vac. Sci.* submitted August 1998.
- Vondrak, R. R., Multiscale Objectives of the Geospace Multiprobes, to appear in *Physics of Space Plasmas*, 15, ed. by T. Chang and J. R. Jasperse, MIT Press, Cambridge, Mass. 1998.
- Wilken, *et al.*, RAPID: The Imaging Energetic Particle Spectrometer on CLUSTER, *Space Sci. Rev.*, 79, 399-473, 1997.
- Wu, C.J., and D.B. Wittry, Investigation of Minority-Carrier Diffusion Lengths by Electron Bombardment of Schottky Barriers, *J. Appl. Phys.*, 49, 2827-2836, 1978.
- Young D.T., *et al.*, 2π Radian Field-of-View Toroidal Electrostatic Analyzer, *Rev. Sci. Instr.* 59, 743-751, 1988.
- Young D.T., *et al.*, Cassini Plasma Spectrometer Investigation, in *Measurement Techniques in Space Plasmas: Particles*, ed. By R.F. Plaff, J.E. Borovsky, and D.T. Young, Amer. Geophys. Union, Wash., DC, 1998.
- Zullinger, H. R., and D. W. Aikten, *IEEE Trans. Nucl. Sci.* NS-17, 39, 1970.

S. M. Ritzau, H. O. Funsten and J. E. Borovsky, Space and Atmospheric Sciences Group, Los Alamos National Laboratory, Los Alamos, NM 87545. (e-mail: sritzau@lanl.gov; hfunsten@lanl.gov; jborovsky@lanl.gov)